JCTC Journal of Chemical Theory and Computation

Time-Dependent Quantum Wave Packet Calculations of Three-Dimensional He − O_2 Inelastic Scattering

Sinan Akpinar, Fahrettin Gogtas,* and Niyazi Bulut

Department of Physics, Faculty Science and Arts, Firat University, Elazig, Turkey

Received February 10, 2005

Abstract: We have studied a three-dimensional time-dependent quantum dynamics of He − O_2 inelastic scattering by using a recently published ab initio potential energy surface. The state-to-state transition probabilities at zero total angular momentum have been calculated in the energy range of 0.12−0.59 eV, and the product rotational distributions are extracted. J-shifting approximation is used to estimate the probabilities for $J > 0$. The integral cross sections and thermal rate constants are then calculated.

1. Introduction

Over the past years, several time dependent quantum wave packet methods were suggested that time dependent quantum approach is quite useful and transparent for studying the dynamics of elementary chemical process, because it allows the direct calculation of observables and shows the possible elementary mechanism.[1] The time-dependent Schördinger equation is initialized from a known quantum state of the system, and the solution of the time dependent Schrödinger equation yields all possible outcomes of interest arising from this initial point. The results for a large range of collision energy can be obtained from a single solution of time-dependent Schrödinger equation.[2] The time dependent approach recently has been used both for two-dimensional and three-dimensional atom−diatom inelastic scattering by many researchers.[3−11]

The He + O_2 may be considered as a prototypical atom−diatom system for low translational energy scattering studies as O_2 is paramagnetic and hence suitable for magnetic trapping method at low energies.[12,13] Therefore, it has been subject to many studies especially concentrated on the rotational alignment and cooling in seeded supersonic expansions of O_2 in He.[14,15] In general, empirical potential energy functions have been employed to investigate this effect. Recently, Groenenboom and Struniewicz[13] have calculated a three-dimensional ab initio ground potential energy surface. Diatomic potential used was constructed from the ab inito calculation and Rydberg-Klein-Rees (RKR) data fitting.[16] Using this full ab inito potential energy surface, the vibrational structure and predissociation dynamics of He + O_2 have been theoretically investigated.[17] Balakrishnan and Dalgarno[18] have carried out the time-independent quantum mechanical calculations to investigate zero temperature quenching rate coefficients for vibrationally and rotationally excited O_2 in collisions with ^{3}He.

In this paper, we discuss a three-dimensional inelastic scattering of He + O_2 by using a grid-based time dependent quantum wave packet method.[2] The paper is organized as follows. In section 2 we discuss the time dependent quantum theory of atom-molecule inelastic scattering. In the last section, the state-to-state inelastic transition probabilities, product rotational distribution, reaction cross sections, and thermal rate constants for the He + O_2 system are discussed.

2. Theory

The method used here is based on the propagation of a state-selected initial wave function in a series of complex Chebychev polynomials and the use of fast Fourier transform,[19] discrete variable representation (DVR),[20] and potentially optimized discrete variable representation techniques[21] for the action of the Hamiltonian operator. The triatomic Hamiltonian operator with total angular momentum $J = 0$ may be written in terms of Jacobi coordinates as

$$\hat{H} = -\frac{\hbar^2}{2\mu}\frac{\partial^2}{\partial R^2} + \frac{\hbar^2 \mathbf{j}^2}{2\mu R^2} + U(R, r, \gamma) + H_{BC}(r) \qquad (1)$$

where R is the distance between the He atom and the center of mass of O_2, r is the O_2 bond length, and γ is the angle between R and r. μ and μ' are corresponding reduced masses, and $\mathbf{j}$ is the rotational angular momentum operator of the O_2 molecule. $H_{BC}(r)$ is the Hamiltonian operator for the diatomic

10.1021/ct050026m CCC: $33.50
Published on Web 11/30/2005

molecule and $U(R, r,\gamma) = V(R, r,\gamma) - V(R = \infty, r, \gamma = 180°)$. As proposed by Kosloff[22] the solution of the time-dependent Schrödinger equation is written in terms of modified complex Chebychev polynomials in the form

$$\psi(R, r, \gamma, t) = e^{-(i/\hbar)(\Delta E/2+V_{min})t}\sum_{n=0}^{N}(2-\delta_{n0}) \times J_n\left(\frac{\Delta E t}{2\hbar}\right)\Phi_n \quad (2)$$

where $\Phi_n = C_n(-i\hat{H}_{norm})\psi(R, r, \gamma, t = 0)$ with $\psi(R, r, \gamma, t = 0)$ being the initial wave function, $C_n(x)$ complex the Chebychev polynomials (CP), $J_n(x)$ the Bessel functions, and ΔE is the magnitude of the entire energy spread of the spectrum of the unnormalized Hamiltonian operator $\hat{H}$. The propagation requires the operation of the $C_n(-i\hat{H}_{norm})$ on ψ. This is performed by using a three-term recursion relation of the Chebychev polynomials

$$\Phi_{n+1} = -2i\hat{H}_{norm}\Phi_n + \Phi_{n-1} \quad (3)$$

The recurrence is started by setting two initial values as $\Phi_o = \psi(R, r, \gamma, t = 0)$ and $\Phi_1 = -i\hat{H}_{norm}\psi(R, r, \gamma, t = 0)$. The initial wave function has three components describing the translational motion of the incoming atom and the vibrational and rotational motions of the target molecule, respectively. The translational wave function has been described in Gaussian form given an initial kinetic energy. The vibrational eigenvalue and eigenfunctions of the diatomic molecule are calculated by solving the time independent Schrödinger equation.[23] The rotational component of the wave function is expressed in associated Legendre polynomials. The action of the Hamiltonian on the wave function in eq 3 is carried out in the following way: Since the potential energy is diagonal in coordinate space, its action on the wave function involves just the multiplication of the values of the potential with those of the wave function at the same spatial grid points. A uniform grid is used for the coordinate R, and the action of the associated kinetic energy operator on the wave packet is evaluated using fast Fourier transforms.[19] The eigenfunctions of the angular kinetic energy operator are known to be the associated Legendre functions $P_j^K(\cos\gamma_l)$ in the general case. For the present application, as J is taken to be zero, normalized Legendre polynomials may be used. Light et al.[20] have discussed the grid or DVR representation based upon a Gauss-Legendre quadrature scheme, and we use this DVR technique for the angular variable γ in the present work. The angular grid points are just the Gauss-Legendre quadrature points. The DVR method allows one to define a transformation matrix which can be used to transform the wave function from the grid (or DVR) representation, in which a value is associated with each grid point $\{\gamma_l, l = 1, 2,.\}$ to a fixed basis representation (FBR) corresponding to an expansion of the wave packet in terms of normalized Legendre polynomials $\hat{P}_j(\cos\gamma_l)$. (Note that $\hat{P}_j$ is used to denote a normalized Legendre polynomial where $\hat{P}_j = \sqrt{(2j+1)/2}P_j$ and P_j is the usual (unnormalized) Legendre polynomial.) The action of the angular part of the kinetic energy operator on the wave function may be easily evaluated when the wave function is expressed as an expansion in Legendre polynomials. This requires the transformation of the wave function from the grid to the FBR representation. The transformation is accomplished by a unitary transformation matrix $\boldsymbol{T}$ defined in terms of normalized Legendre polynomials as $T_{j,l} = \omega_l^{1/2}\hat{P}_j(\cos\gamma_l)$. If an N_γ Gauss-Legendre quadrature scheme is used, then the maximum value of j in the associated fixed basis representation (FBR) is $j_{max} = (N_\gamma - 1)$. In the FBR representation the action of the angular part of the kinetic energy operator on the wave function is accomplished by simply multiplying by $j(j + 1)/2I$. The final DVR wave function is then obtained by carrying out an inverse transformation from the FBR to the grid or DVR representation. This inverse transformation is carried out by using the Hermitian conjugate of the matrix $\boldsymbol{T}$. The action of diatomic Hamiltonian operator is performed by using a potentially optimized discrete variable representation technique which we described in our previous study.[7]

In numerical evaluation for atom−diatom inelastic scattering, the initial wave packet is located in the asymptotic region of entrance channel and propagated on the potential energy surface toward the strong interaction region. In this work we wish to compute state-to-state inelastic scattering probabilities and must therefore follow the development of the wave packet being reflected from the interaction region. Our method of extracting the state-to-state reaction probabilities from the wave packet dynamics requires us to analyze the wave packet as it passes a line in the asymptotic region. To extract the cross section and other observable quantities from the wave packet dynamics, the wave packet is analyzed at each time step by taking cuts through at a fixed value of the scattering coordinate $R = R_\infty$

$$C_{v'j'}(t) = \int_{r=0}^{\infty}(\sum_k \psi(R_\infty, r, \gamma_k, t)P_{j'}(\gamma_k)\omega_k)\phi_{v'j'}(r)dr \quad (4)$$

where ω_k are the weights in Gauss Quadrature formula.[2] The transition probabilities for the production of specific final vibrational−rotational states from a specified initial reactant level are given by[24]

$$P_{jv,v'j'}(E) = \frac{\hbar^2}{\mu\mu'}k_{v'j'}k_{jv}|\frac{A_{v'j'}(E)}{f(k)}|^2 \quad (5)$$

where $A_{v'j'}(E)$ are the Fourier transform of time dependent coefficients ($C_{v',j'}(t)$). k_{jv} is related to total energy E and rovibrational energy states of the diatomic molecule, ϵ_{jv}, by

$$k_{jv} = \left[\frac{2\mu(E-\epsilon_{jv})}{\hbar^2}\right]^{1/2} \quad (6)$$

In applying the time-dependent quantum methods to scattering problems one is always faced with numerical difficulties associated with the reflection of the wave function from the end of the grid. This artificial boundary reflection is due to the discretization of the continuum space by a finite space. Therefore, the wave packet after being analyzed has to be disposed of before reaching the edges of the grid. At present calculations, a negative complex damping potential with aquadratic form has been used at both edges of the grid. For this reason, the normalized Hamiltonian operator is given in eq 3

$$H_{\text{norm}} = H_{\text{norm}} - iA_R\left[\frac{R_d - R}{R_{\max} - R}\right]^2 - iA_r\left[\frac{r_d - r}{r_{\max} - r}\right]^2 \quad (7)$$

where R_d and r_d are the starting points of the complex damping potential, $R_{\max}$ and $r_{\max}$ are the maximum lengths of the grids, and A_R and A_r are the absorbing potential parameters in R and r, respectively. The range of the damping function is limited only in the damping region. That is, when $R < R_d$ the absorbing potential is taken as zero (same reads when $r < r_d$). To prevent any reflection either from the edges of the grid or from the damping potential itself the absorbing potential not to cause any instability, the absorbing potential parameters are optimized as instructed by Vibok and Balint−Kurti.[25] On the other hand, the Bessel functions play a very important role in the convergence of the CP expansion. The number of terms to be used in the CP expansion is set equal to the argument of the Bessel functions which is given in terms of the energy range of the Hamiltonian as $\Delta Et/2\hbar$. Bessel functions decrease exponentially to zero for n values greater than their argument. Therefore, the CP expansion will be unstable if the energy range of the Hamiltonian operator is underestimated. Despite all these precautions we follow the norm of the wave packet at each time step to make sure that the expansion is stable during the propagation. The calculation of the total crosssections requires having the reaction probabilities for all available J values.

$$\sigma_{v,j}(E) = \frac{\pi}{k_{v,j}^2}\sum_{J=0}^{\infty}(2J+1)P_{jv,v'j'}^{J}(E) \quad (8)$$

One approximate way to estimate the reaction probabilities for $J > 0$ is to use the J-shifting method.[26,27] In the J-shifting method the total reaction probabilities for $J > 0$ are calculated by using

$$P^J(E) = P^{J=0}(E - E_{\text{shift}}^J) \quad (9)$$

where $P^{J=0}(E)$ is the accurately computed reaction probability for $J = 0$, at the total energy E, and $P^J(E)$ is the estimated reaction probability for another value of J. The shifting energy is defined as[26,27]

$$E_{\text{shift}}^J = \frac{\hbar^2 J(J+1)}{2\mu R^2} \quad (10)$$

The state-to-state rate constant can be calculated by Boltzmann averaging of the integral crosssection over the collision energy[28]

$$k_{v,j}(E_C) = \frac{d_f}{k_B T}\left(\frac{8}{\pi\mu_{A+BC}k_B T}\right)^{1/2} \times \int dE_C E_C e^{-E_C/k_B T}\sigma_{v,j}(E_C) \quad (11)$$

where d_f is the electronic degeneracy factor,[28] k_B is the Boltzmann constant, and $E_C = E - \epsilon_{v,j}$ is the collision energy.

3. Results and Discussion

In this section, the theory described above was applied to compute rovibrational transition probabilities in inelastic scattering of He + O_2 ($v = 0$, $j = 0$, 1, 2). The potential energy surface has a local minimum of $0.001167a_o$ at a linear geometry, $r = 2.282a_o$, $R = 6.9a_o$. The sattle point with the energy of 0.000368 above the global minimum is located at $R = 6.9a_o$. The coordinate grid used for the propagation covers He − O_2 separations from $2.76a_o$ to $48.3a_o$ and O−O separations from $0.6846a_o$ to $6.846a_o$. 512 evenly spaced grid points were used in the R. The potentially optimized discrete variable representation (DVR) technique is used to set up r grid points and related basis functions, which then allows a compact grid-based matrix representation of diatomic Hamiltonian operator. 32 potentially optimized r grid points were used in the calculations. The maximum value of the rotational quantum number used in the expansion of the wave function (designated $j_{\max}$) was set equal to 60, which allows for several closed channels at the highest energies in the wave packet. The initial wave packet was centered around a He − O_2 separation of $27.57a_o$ and given a kinetic energy of 0.02 eV along the entrance valley. The wave packet had an effective range of kinetic energy from 0.12 to 0.59 eV.

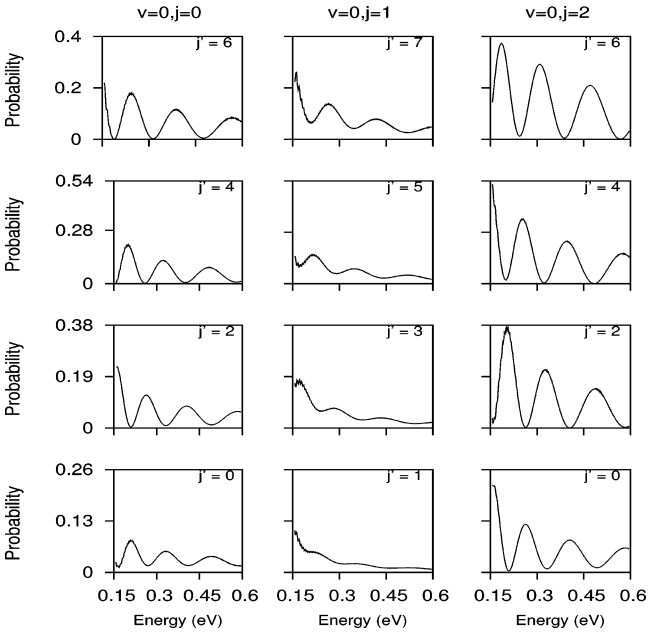

Figure 1. The inelastic transition probabilities for He + O_2($v = 0$, j) → He + O_2($v' = 0$, j') with $j = 0,1,2$.

The time step used for the propagation was approximately 1.2 fs. This small time step leads the wave packet to have a translational energy range of 0.12−0.59 eV. An analysis plane is located at a He − O_2 separation of $34.5a_o$. This plane is defined to lie perpendicularly across the asymptotic region. At each time step, a cut is taken through the wave packet along this plane, and the resulting two-dimensional wave function is analyzed into its fragment state contribution. The analysis of the wave packet as it passes the analysis plane yields the time dependent coefficients. The propagation is continued until all the wave packet has completely left the interaction region, in which case the time dependent coefficients decrease to zero. The portions of the wave packet reflected back into the reaction channel will eventually reach the edge of the numerical grid. If no special precautions are taken, the parts of the wave packet that reach the edge of the grid will be unphysically reflected back onto the grid,

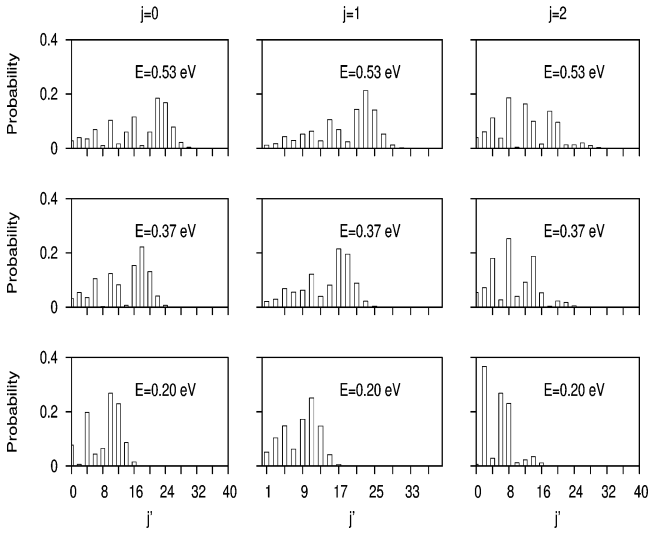

Figure 2. Product rotational distributions at fixed energy values.

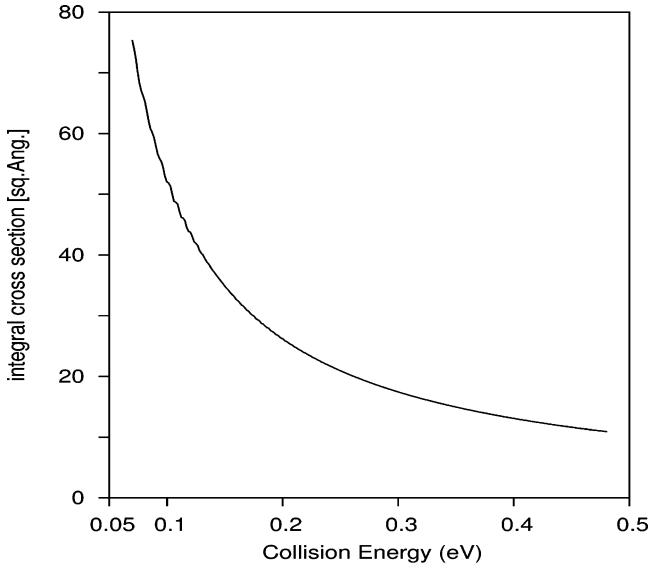

Figure 3. Integral cross sections as a function collision energy for O_2 in its ground.

invalidating the results of the calculations. To avoid such a reflection the damping potential (eq 7) was employed at both edges of the grid at $R_d = 38.58a_o$ and $r_d = 5.22a_o$.

Figure 1 shows the calculated inelastic transition probabilities as a function of translational kinetic energy. As seen from the figure, the individual transition probabilities shows broad oscillatory structures as a function of collision energy. That is, an edge is followed by a monotonic decline. Since the potential energy surface is fully repulsive and has a deep well, this oscillatory feature of the transition probability is attributed to rainbow in the scattering as explained in details by Schinke et al.[29,30] and Levine et al.[31] The state-resolved transition probabilities decrease with increasing energy and have a tendency for even−odd alternation according to the parity selection rule. That is, there is no transition between the even and odd quantum states.

The final rotational distributions for O_2 initially in its ground and first two rotationally excited states are shown in Figure 2 for three different total energy values (0.20, 0.37, 0.53 eV). The rotational distributions show again a rainbow-like structured shape with clear dependency to final rotational quantum number. On the other hand, it may be seen that the shape of the distributions changes as the collision energy increased. That is, the maximum peak of the distribution shifts to higher j' as the translational energy increased, indicating also the energy dependency of rotational distributions.

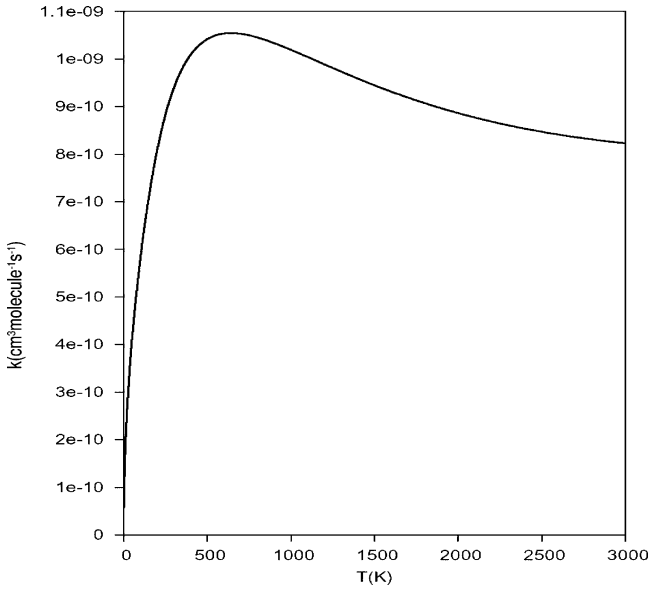

Figure 4. Thermal rate constants derived from the reaction cross sections in Figure 3.

Figure 3 shows the integral cross sections, or excitation functions, corresponding to the O_2 in ground state. The integral cross section has no threshold and is seen to decrease with increasing collision energy. The cross section is very large near zero collision energy and decreases sharply with increase in energy. The thermal rate constants are displayed in Figure 4 for the O_2 in ground state. The rate constants show a weak temperature dependence as it is expected for the reaction with a deep well and high barrier.

References

(1) Defazio, P.; Petrongolo, C. *J. Theor. Comput. Chem.* **2003**, *2*, 547.

(2) Gögtas, F.; Balint-Kurti, G. G.; Offer, A. R. *J. Chem. Phys.* **1996**, *104*, 7927.

(3) Skouteris, D.; Lagana, A.; Capecchi, G.; Werner, H.-J. *Int. J. Quantum Chem.* **2004**, *96*, 547.

(4) Gogtas, F.; Bulut, N.; Oturak, H.; Kökce, A. *J. Mol. Struct. (THEOCHEM)* **2002**, *584*, 149.

(5) Bradley, K. S.; Schatz, G. C.; Balint-Kurti, G. G. *J. Phys. Chem. A* **1999**, *103*, 947.

(6) Akpinar, S.; Gogtas, F.; Bulut, N.; Yildiz, A. *Int. J. Quantum Chem.* **2000**, *79*, 274.

(7) Gogtas, F.; Bulut, N. *Mol. Phys.* **2002**, *100*, 561.

(8) Zhang, D. W.; Wang, M. L.; Zhang, John Z. H. *J. Chem. Phys.* **2003**, *118*, 2716.

(9) Lin, S. Y.; Guo, H. *J. Chem. Phys.* **2003**, *119*, 11602.

(10) Palov, A. P.; Jimeno, P.; Gray, M. D.; Balint-Kurti, G. G. *J. Chem. Phys.* **2003**, *119*, 11602.

(11) Akpinar, S.; Bulut, N.; Gogtas, F. *J. Theor. Comput. Chem.* **2004**, *3*, 291.

(12) Doyle, J. M.; Friedrich, B.; Kim, J.; Patterson, D. *Phys. Rev. A* **1995**, *52*, R2515.

(13) Groenenboom, G. C.; Struniewicz, I. M. *J. Chem. Phys.* **2000**, *121*, 9562.

(14) Aquilanti, V.; Ascenzi, D.; de Castro Vitores, M.; Pirani, F.; Cappeletti, D. *J. Chem. Phys.* **1999**, *111*, 2620.

(15) Fair, J. R.; Nesbitt, D. J. *J. Chem. Phys.* **1999**, *111*, 6821.

(16) Babb, J. F.; Dalgarno, A. *Phys. Rev. A* **1995**, *51*, 3021.

(17) Jung, J.; Sun, H. *Mol. Phys.* **2001**, *99*, 1867.

(18) Balakrishnan, N.; Dalgarno, A. *J. Phys. Chem.* **2001**, *105*, 2348.

(19) Kosloff, R.; Cerjan, C. *J. Chem. Phys.* **1984**, *81*, 3722.

(20) Light, J. C.; I. Hamilton, P.; Lill, V. J. *J. Phys. Chem.* **1985**, *82*, 1400.

(21) Balint-Kurt, G. G.;, Pulay, P. *J. Mol. Struct. (THEOCHEM)* **1995**, *341*, 1−11.

(22) Tal-Ezer, H.; Kosloff, R. *J. Chem. Phys.* **1984**, *81*, 3967.

(23) Gögtas, F.; Balint-Kurti, G. G.; Marston, C. C. Quantum Chemistry Program Exchange, Program No. 647; QCPE Bulletin, 1994; Vol. 14, p 19.

(24) Balint-Kurti, G. G.; Dixon, R. N.; Marston, C. C. *Faraday Trans. Chem. Soc.* **1990**, *86*, 1741.

(25) Vibok, A.; Balint-Kurti, G. G. *J. Phys. Chem.* **1992**, *96*, 8712.

(26) Bowman, J. M. *J. Phys. Chem.* **1991**, *95*, 4960.

(27) Bittererova, M.; Bowman, J. M. *J. Chem. Phys.* **2000**, *113*, 1.

(28) Lin, S. Y.; Guo, H. *J. Chem. Phys.* **2005**, *122*, 74304.

(29) Schinke, R. *J. Chem. Phys.* **1980**, *72*, 1120.

(30) Mller, W.; Schinke, R. *J. Chem. Phys.* **1981**, *75*, 1219.

(31) Levine, R. D.; Bernstein, R. B. *Molecular Reaction Dynamics and Chemical Reactivity*; Oxford University Press: 1987.

CT050026M